

行政院國家科學委員會專題研究計畫 期中進度報告

5~6 GHz 频段室內寬頻 / 超寬頻無線通道量測與模擬 (2/3)

計畫類別：個別型計畫

計畫編號：NSC92-2213-E-009-047-

執行期間：92年08月01日至93年07月31日

執行單位：國立交通大學電信工程學系

計畫主持人：唐震寰

報告類型：精簡報告

處理方式：本計畫可公開查詢

中 華 民 國 93 年 5 月 26 日

5~6 GHz 頻段室內寬頻 / 超寬頻無線通道量測與模擬(2/3)

5~6 GHz Wideband / Ultra-wideband Radio Measurement and Channel Modeling for Indoor Environments (2/3)

計畫編號：NSC91-2213-E009-128

執行期限：92 年 8 月 1 日至 93 年 7 月 31 日

主持人：唐震寰 國立交通大學電信工程學系

中文摘要

超寬頻無線技術由於其高傳輸容量、不易受多重路徑影響、具備精密的定位及測距能力、以及不易被截取等優點，近年來在科學、工業、通信及軍事等領域上都獲得相當大的重視，歐美各國也都相繼投入其應用研發。為瞭解超寬頻信號在室內的通道特性，本計畫乃規劃以掃頻量測方法，量測及探討其室內傳播特性。本計畫將於三年內進行兩階段之研究工作：(1) 第一階段(第一及第二年)：對超寬頻信號傳播路徑損耗、衰落、及功率延遲分佈等特性進行量測與模型建構及驗證；(2) 第二階段(第三年)：以第一階段的研究結果應用於在探討超寬頻信號在室內無線傳播特性。

在計畫執行的第一年中，我們完成了超寬頻室通道量測系統的架設，以此系統對 5 ~ 6 GHz 寬頻信號在室內的傳播特性進行量測。同時，也以所發展的三維適應環境性傳播模型及射線追蹤技術來模擬此一頻段的無線信號在室內環境的傳播現象。為能獲得較合理的模擬結果，研究中同時也對一般室內建材在超寬頻頻段的介電係數進行量測，並將所測得的介電係數用於模擬中。經比較量測與模擬所得的數據，証實了此傳播模型之有效性與正確性。

本年度為計畫執行的第二年，我們以預估延遲拍線模型為基礎，對室內超寬頻信號功率延遲分佈的相關參數如時間延遲係數和功率損耗率等進行分析。同時也推導出時間延遲係數和功率損耗率與信號頻寬的關係式，可用以預測室內環境中不同頻寬信號的功率延遲分佈特性。研究中也以所架設之超寬頻脈衝響應量測系統，在不同條件的室內環境下進行了大量的量測。經與量測結果比較後，也驗證了所推導模型的正確性，並且得到兩項結果：(1) 同一傳播環境中，信號的頻寬並不會對平均功率延遲分佈的時間延遲係數造成影響；(2) 同一傳播環境中，平均功率延遲分佈的功率損耗率會隨著信號頻寬的增加而減少。

關鍵詞：超寬頻、功率延遲分佈、預估延遲拍線模型

Abstract

Ultra Wideband (UWB) radio techniques have recently attracted great interest in scientific, industrial, commercial, and military sectors. The potential strength of the UWB radio technique such as high channel capacity at short range, lack of significant multipath fading, accurate position location and ranging, and extremely difficult to intercept, lies in its use of extreme wide transmission bandwidths.

In this project, a spectrum analyzing and a

swept frequency measurement methods are adopted to measure and to analyze the UWB radio propagation loss, multi-path fading, signal delay and spread. It is a three years project and is separated into two stages. (1) The first stage (1st and 2nd years): measurement and modeling of the UWB radio propagation loss, multi-path fading, and power delay profile; (2) The second stage (3rd year): investigation of UWB indoor propagation characteristics.

In the last annual report, an ultra wideband channel sounding system and a swept frequency measurement method are adopted to measure and to analyze UWB radio wave propagation characteristics in indoor environment. A site-specific model using ray-tracing technique is developed to predict the radio propagation in indoor environments. Simulation results are validated by the experimental results.

In this year, the stochastic tapped-delay-line (STD-L) model is introduced to model the UWB indoor channels with the parameters, delay constant and power ratio, of the averaged power-delay profile (PDP). Here, the formulas of these two parameters versus signal bandwidth are proposed. The formulas have been validated by comparing the computed results with a large number of measurement data carried out at many sites such as classrooms, laboratories and offices. The measured frequencies are ranged from 3 GHz to 5 GHz. It is found that (1) The delay constant of the averaged PDP is independent of radio bandwidth; (2) The power ratio of the averaged PDP is decreased when the radio bandwidth is increased.

Keywords: Ultra wideband, power-delay profile, stochastic tapped-delay-line model.

I. Introduction

Ultra Wideband (UWB) radio techniques have recently attracted great interest in scientific, industrial, commercial, and military sectors. The potential strength of the UWB radio technique such as high channel capacity at short range, lack of significant multipath fading, accurate position location and ranging, and extremely difficult to intercept, lies in its use of extreme wide transmission bandwidths. According to the Federal Communication Commission (FCC)

regulations of UWB radio technology and systems [1], minimum bandwidth limit of an UWB radio signal is 500 MHz, and the frequency band from 3.1 GHz to 10.6 GHz is allowed for unlicensed use for indoor communication applications.

Currently, standards adapting UWB radio technology are under developing. The IEEE 802.15 task group TG3a [2] is developing a high rate alternative physical (PHY) to support high rate applications such as imaging and multimedia for wireless personal area network (WPAN) by exploiting the advantages of the UWB-radio's high capacity. In addition, the IEEE 802.15 study group SG4a [3] is developing a low rate alternative PHY to support high precision ranging/location capability for WPAN by exploiting the advantages of the UWB-radio's fine time resolution. However, the UWB technology is not yet fully developed, and the efficient design of such communication systems require new experimental and theoretical activities. In particular, an appropriate channel model that accurately describes the UWB propagation is needed.

In this project, a spectrum analyzing and a swept frequency measurement methods are adopted to measure and to analyze the UWB radio propagation loss, multi-path fading, signal delay and spread. It is a three years project and is separated into two stages. (1) The first stage (1st and 2nd years): measurement and modeling of the UWB radio propagation loss, multi-path fading, and power delay profile; (2) The second stage (3rd year): investigation of UWB indoor propagation characteristics. In the last annual report [4], an ultra-wide band channel sounding system and a swept frequency measurement method are adopted to measure and to analyze UWB radio wave propagation characteristics in indoor environment. A site-specific model using ray-tracing technique is developed to predict the radio propagation in indoor environments. Simulation results are validated by the experimental results.

In this paper, a model is introduced to modeling the multipath power-delay profile (PDP) of UWB indoor channels. Due to the extreme wide radio bandwidth, UWB systems achieve very high multipath resolution. For a typical indoor environment, the UWB channel response usually contains several tens to hundreds multipath components. These properties make UWB channels very different from those of narrow band systems, and these are roots of many characteristics of UWB systems. Therefore, thorough understanding and precise modeling of the multipath PDP is of primary importance to the

UWB channel model. Many propagation measurements have been performed for indoor UWB channels and several PDP models have been proposed in the literature [5]-[7]. For examples, [8] uses an extension of the D-K model [5] to a delay resolution of 5ns. The result of [9]-[11] shows that the S-V model [6] is well to characterize the UWB indoor channel. Both the D-K and S-V models are familiar to characterize the multipath clustering phenomenon. Another well-validated model is stochastic tapped-delay-line (STDL) model [7]. It models the PDP by a single exponential decay with time delay.

In previous researches, the dependence of propagation environment, T-R separation, carrier frequency and some other factors on the PDP of UWB channels have been investigated. However, to the best of the authors' knowledge, few researches focused on the studies of the effect of radio bandwidth on propagation channel model so far. It is noted that according to the FCC regulation of UWB radio technology and systems, the UWB radio bandwidth that affects the multipath resolution may vary in a wide range from several hundred MHz to a few GHz to provide manifold applications with varying data rate and quality of services (QoS) requirements.

From our measurement and analysis results, the STDL model is introduced to model the multipath PDP of UWB indoor channels in this paper. All the parameters of the STDL model for several radio bandwidths ranging from 500 MHz to 2 GHz have been extracted from a set of measured impulse responses. The effect of radio bandwidth on those parameters is analyzed theoretically and validated by measurement results. By using our derived results, it is simple to calculate the channel parameters for different radio bandwidth if we know those of one specific radio bandwidth. It is helpful to provide proper multipath PDP models for the simulation and evaluation of UWB systems with different radio bandwidth.

II. STDL Channel Model

The STDL model characterizes the shape of the PDP of the UWB indoor channel in terms of path power and delays of a subsequent discrete taps with equal time spacing, i.e., by the pairs $\{P_k, \tau_k\}$ with $\tau_k = (k-1)\tau$, where τ is the tap spacing which is inversely proportional to the radio bandwidth of the considered system. Therefore, the power of each tap, G_k , results from the square of the sum of the complex fields of multipath components (MPCs) arriving within τ of the corresponding bin varies rapidly.

From our measurement and analysis results

as shown in Figure 1, it is found that the average power of the subsequent taps, \bar{P}_k , decay exponentially (linearly on a decibel scale) with delay starting from the second bin, and may be expressed as

$$\begin{aligned} \bar{P}(\tau) &= \sum_{k=1}^N \bar{P}_k \delta(\tau - \tau_k) \\ &= \bar{P}_1 \left\{ \delta(\tau - \tau_1) + \sum_{k=2}^N r \exp\left(-\frac{(\tau_k - \tau_1)}{\epsilon}\right) \delta(\tau - \tau_k) \right\} \end{aligned} \quad (1)$$

where N is the total number of bins in the observation window, r is the ratio of the average power of the second tap to the first tap, and ϵ is the exponentially power decay constant. For the convenience of description in the following of this paper we refer to r and ϵ as the power ratio and decay constant, respectively. It is noted that, \bar{P}_k are normalized to the power of the first tap, and τ_k are translated to the delay of the first tap, i.e., $\bar{P}_1 = 1$ and $\tau_1 = 0$.

These parameters r and ϵ are not only dependent on the propagation environment and maybe dependent on the radio bandwidth of the considered system.

III. Effect of Radio Bandwidth on Parameters of STDL Model

Due to the extreme wide transmission radio bandwidth, UWB systems achieve very high multipath resolution. Because the resolution is inversely proportional to the radio bandwidth of the considered system, it is expected that the characteristics of an UWB propagation channel is significant dependent on the radio bandwidth. Figures 2(a) and (b) show the PDP diagrams for UWB channels with radio bandwidth F and $f=F/2$, respectively.

From Equation (1), the average power of each tap, \bar{P}_j^F , for signal with radio bandwidth F , and \bar{P}_i^f for signal with radio bandwidth f , can be expressed as Equations (2) and (3), respectively.

$$\begin{cases} \bar{P}_1^F = 1 \\ \bar{P}_j^F = r^F \times \exp\left[-\frac{(j-2) \times \Delta^F}{\epsilon^F}\right], & j \geq 2 \end{cases} \quad (2)$$

$$\begin{cases} \bar{P}_1^f = 1 \\ \bar{P}_i^f = r^f \times \exp\left[-\frac{(i-2) \times \Delta^f}{\epsilon^f}\right], & i \geq 2 \end{cases} \quad (3)$$

For an uncorrelated scattered radio propagation channel [12], the amplitudes of the taps fluctuate independently of each other. From our measurement results shown in Section V and that in [7], it reveals that the uncorrelated scattering assumption can be applied to the indoor UWB radio propagation channels. Therefore, \bar{P}_i^F can be calculated as the sum of \bar{P}_{2i-1}^F and \bar{P}_{2i}^F , and is given by

$$\begin{cases} \bar{P}_1^f = \bar{P}_1^F + \bar{P}_2^F = 1 + r^F \\ \bar{P}_i^f = \bar{P}_{2i-1}^F + \bar{P}_{2i}^F \\ = r^F \times \left\{ \exp\left[-\frac{(2i-3) \times \Delta^F}{\epsilon^F}\right] \right. \\ \left. + \exp\left[-\frac{(2i-2) \times \Delta^F}{\epsilon^F}\right] \right\} \\ = r^F \times \left[\exp\left(-\frac{\Delta^F}{\epsilon^F}\right) + \exp\left(-\frac{2 \times \Delta^F}{\epsilon^F}\right) \right] \\ \times \exp\left(-\frac{(i-2) \times 2 \times \Delta^F}{\epsilon^F}\right), & i \geq 2 \end{cases} \quad (4)$$

Comparing Equations (3) and (4), it is found that the decay constant is not dependent on the radio bandwidth since ϵ^f and ϵ^F are equal. It is also found that r^f can be determined by r^F , ϵ^F and Δ^F by Equations (5).

$$\begin{aligned} r^f &= \frac{r^F}{1 + r^F} \times \left[\exp\left(-\frac{\Delta^F}{\epsilon^F}\right) + \exp\left(-\frac{2 \times \Delta^F}{\epsilon^F}\right) \right] \\ &\approx \frac{2 \times r^F}{1 + r^F}, \quad \text{if } \Delta^F \ll \epsilon^F \end{aligned} \quad (5)$$

From Equation (5), it is found that r^f is greater than r^F under the condition that if $\epsilon^F \gg \Delta^F$. The indoor UWB channels, for the most part, satisfy this condition with a typical decay constant larger than 20ns and tap spacing smaller than 2ns.

From Equation (5) and the condition $\epsilon^F = \epsilon^f$, it is also found that r^f can be determined by r^F , ϵ^F and Δ^F by Equation (6)

$$\begin{aligned} r^F &= \frac{r^f}{\left[\exp\left(-\frac{1/2 \times \Delta^f}{\epsilon^f}\right) + \exp\left(-\frac{\Delta^f}{\epsilon^f}\right) \right]} - r^f \\ &\approx \frac{r^f}{2 - r^f}, \quad \text{if } \Delta^f \ll \epsilon^f \end{aligned} \quad (6)$$

To sum up, among these parameters of STDL multipath PDP model, the power ratio r is dependent on the radio bandwidth, but the decay constant is not. If we know those parameters of one specific radio bandwidth, then Equation (5) can be used to estimate that for a narrower radio bandwidth, and Equation (6) for estimation of that for a wider radio bandwidth.

IV. Measurement Setup and Environment

In our study, the frequency domain measurement technology to perform UWB indoor channel sounding is adopted. A schematic diagram of the measurement system is shown in Figure 3. An Agilent 8719ET Vector Network Analyzer (VNA) was used for measuring the frequency response of the channel. The transmitted signal is sent from the VNA to the transmitting antenna through a low-loss 10-m coaxial cable. Both the transmitting and receiving antennas, EM-6865, are vertically polarized and omni-directional (in the H-plane). The signal from the receiving antenna is first through a Low Noise Amplifier (LNA) with a gain of 30 dB. It is then returned to the VNA via a low-loss 30-m coaxial cable. The VNA records the variation of 801 complex tones across the 3-5 GHz frequency range, by measuring the S-parameter, S_{21} , of the UWB channel, which is essentially the transfer function of the channel. The time-domain channel response can be obtained by taking the inverse Fourier transform of the frequency-domain channel response.

It is noted that the frequency range of our experiment is only focus on 3 to 5 GHz, not the full range that allocated by FCC. It is because that 3 to 5 GHz is the primary band that IEEE 802.15.3a standard focused. At present, there are two PHY proposals for IEEE 802.15.3a, one is so-called DS-UWB and the other is Multi-band OFDM. In DS-UWB proposal [13], UWB systems operate in two different bands, one band nominally occupying the spectrum from 3.1 to 4.85 GHz (the low band), and the second band occupying the spectrum from 6.2 to 9.7 GHz (the high band). A compliant UWB radio device is required to implement only support the low band. In Multi-band OFDM proposal [14], it divides the spectrum into several 528 MHz bands, and groups the bands into 5 distinct groups. One of the groups, 3.168-4.752 GHz, that contains three 528 MHz bands is mandatory, and the remaining 4 groups are optional.

UWB propagation experiments were performed in a laboratory/education building at

the National Chiao-Tung University in Hsin-Chu, Taiwan. The floor plan is shown in Figure 4. Both Line-of-Sight (LOS) and non-LOS (NLOS) propagations were considered for measurements. As shown in Figure 4, there are 9 measured points for UWB measurement. Rxs.1-3 were under the LOS condition (Site A), Rxs.4-6 were under the NLOS condition with short T-R separation (Site B), Rxs.7-9 were also under the NLOS condition but with long T-R separation (Site C). In each measurement, both the transmitting and receiving antenna were fixed with the same height of 1.6m. At each measured point, channel frequency responses were sampled at 64 measurement subpoints, arranged in a fixed-height, 8×8 square grid. The spacing between two neighboring subpoints is 3.75cm. Therefore, a total number of 576 channel frequency responses were recorded.

V. Validation and Discussion

We processed all the measured frequency-domain channel responses to time-domain by taking the inverse Fourier transform. Since the absolute propagation delays of the received signals vary from one point to another, an appropriate delay reference is needed to characterize the relative delays of each MPC. Here we translate the delay axis of the PDP for each measurement point by its respective absolute delay of the directed path between transmitter and receiver.

For each measurement point, PDPs of the 64 subpoints were normalized to the average of these 64 PDPs to remove the large-scale path loss. Therefore, 3×64 normalized PDPs were collected to get an averaged PDP for each measurement site. Then the parameters, decay constant and power ratio for each measurement site are extract by best-fit procedures, and listed in Tables I and II, respectively.

From Table I, it is found that the decay constant varies from site to site but tends to be a fixed value for different radio bandwidth. This validates our finding that the decay constant is not dependent on the radio bandwidth. From Table II, it is found that the power ratio is decreased when the radio bandwidth increased which validates our analyzed results in section III.

VI. Conclusion

A STDL model is introduced to model the multipath power-delay profile of UWB indoor channels. The parameters of the STDL model such as decay constant ϵ and power ratio for radio bandwidths of 500 MHz, 1 GHz, 1.5 GHz, and 2

GHz have been extracted from a set of measured impulse responses. The effect of radio bandwidth on these parameters is analyzed theoretically. Measurement results show that the decay constant ε is independent of the radio bandwidth, while the power ratio r is decreased with the increased radio bandwidth. These results validate the STDL model in multipath power-delay profile analyze of UWB indoor propagation.

The relations of the decay constant and power ratio for UWB radio wave with different bandwidth are also derived in this paper. These equations can be use to predict the channel parameters for different radio bandwidth once the parameters of one specific radio bandwidth are obtained. This is helpful for the simulation and evaluation of UWB systems with different radio bandwidth.

References

- [1] FCC "Revision of Part 15 of the Commission's Rules Regarding Ultra-Wideband Transmission Systems," First Report and Order, ET Docket 98-153, FCC 02-48, Apr. 2002.
- [2] IEEE 802.15 Wireless Personal Area Network High Rate Alternative PHY Task Group 3a (TG3a), <http://www.ieee802.org/15/pub/TG3a.html>
- [3] IEEE 802.15 Wireless Personal Area Network Low Rate Alternative PHY Study Group 4a (SG4a), <http://www.ieee802.org/15/pub/SG4a.html>
- [4] J. H. Tarng, "5~6 GHz Wideband / Ultra-wideband Radio Measurement and Channel Modeling for Indoor Environments (1/3)," Annual report 91 of Project NSC91-2213-E009-128, May 2003.
- [5] H. Hashemi, "Impulse Response Modeling of Indoor Radio Propagation Channels," IEEE Journal on Selected Areas in Communications, vol. 11, no. 7, Sep. 1993, pp. 967-978.
- [6] A. Saleh and R. Valenzuela, "A Statistical Model for Indoor Multipath Propagation," IEEE Journal on Selected Areas in Communications, vol. SAC-5, no. 2, Feb. 1987, pp. 128-137.
- [7] Dajana Cassioli, Moe Z. Win, Andreas F. Molisch, "The Ultra-Wide Bandwidth Indoor Channel: From Statistical Model to Simulations ", IEEE Journal on Selected Areas in Communications, vol. 20, no.6, Aug. 2002, pp. 1247-1257.
- [8] J. Foerster, "The Effects of Multipath Interference on the Performance of UWB Systems in an Indoor Wireless Channel," IEEE Semiannual Vehicular Technology Conference, Rhodes, Greece, May 2001, pp. 1176-1180.
- [9] Q. Spencer, B. Jeffs, M. Jensen, and A. Swindlehurst, "Modeling the Statistical Time and Angle of Arrival Characteristics of an Indoor Multipath Channel," IEEE Journal on Selected Areas in Communications, vol. 18, no. 3, Mar. 2000, pp. 347-360.
- [10] R. J.-M. Cramer, R. A. Scholtz, and M. Z. Win, "Evaluation of an Ultra-Wide-Band Propagation Channel," IEEE Transactions on Antennas and Propagation, vol. 50, no. 5, May 2002, pp. 561-570.
- [11] J. Foerster, and Q. Li, "UWB Channel Modeling Contribution from Intel," described in document IEEE P802.15-02/279r0-SG3a.
- [12] J. D. Parsons, "The Mobile Radio Propagation Channel," Pentech Press Publishers, London, 1992.
- [13] "DS-UWB Physical Layer Submission to 802.15 Task Group 3a," described in document IEEE P802.15-04/0137r0, Mar. 2004.
- [14] "Multi-band OFDM Physical Layer Proposal Update," described in document IEEE 802.15-04/0122r4, Mar. 2004.

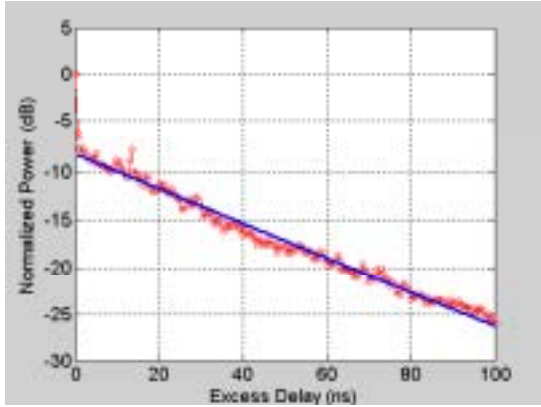


Fig. 1. One sample of the average delay profile versus the excess delay. The wavy line is the measured profile, the straight line is the exponential decay obtained by a best-fit procedure.

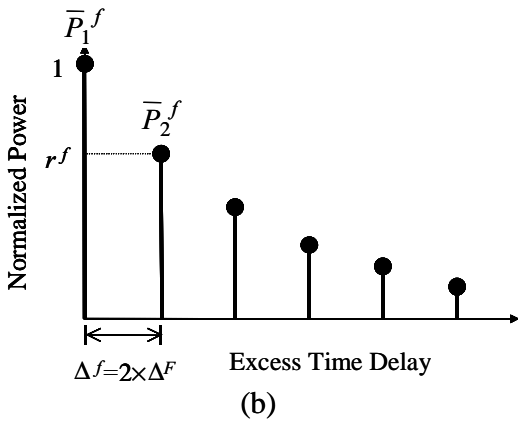
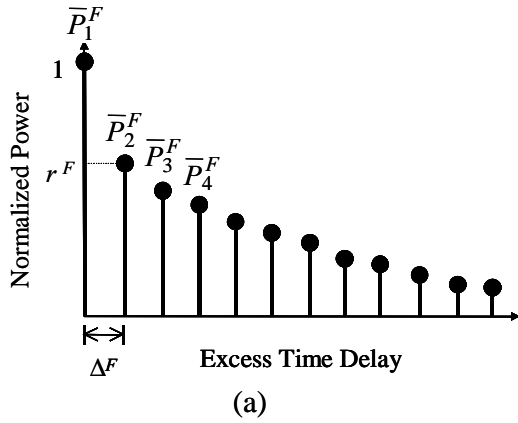


Fig. 2. Diagrams of UWB channel PDPs with radio bandwidth (a) F ; and (b) $f=F/2$.

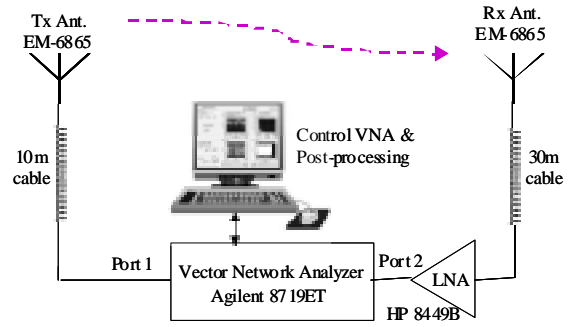


Fig. 3. Schematic diagram of the UWB indoor channel measurement system.

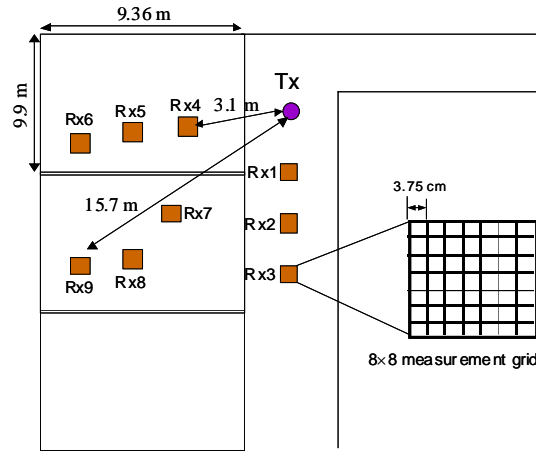


Fig. 4. The floor layout of the laboratory/education building where the UWB indoor channel measurement was performed.

Table I. Decay constant ϵ of the measurement sites (unit:ns)

Bandwidth Sites	500 MHz	1 GHz	1.5 GHz	2 GHz
Site A	15.5	14.4	15.2	15.8
Site B	14.0	13.0	12.9	13.1
Site C	19.0	18.5	20.2	20.4

Table II. Power ratio r of the measurement sites

Bandwidth Sites	500 MHz	1 GHz	1.5 GHz	2 GHz
Site A	0.0777	0.0372	0.0194	0.0128
Site B	0.0650	0.0325	0.0217	0.0150
Site C	0.2340	0.1080	0.0633	0.0440